Water and energy budget of the Ohrid Lake basin for 1990: Part A) Water and energy budget of a land site near the lake – the Ohrid...

Eram Artinyan
Bulgarian Academy of Sciences

Water and energy budget of the Ohrid Lake basin for 1990: Part A) Water and energy budget of a land site near the lake – the Ohrid meteorological station; Part B) Estimation of the lake monthly water budget for 1990;

E. Artinyan[a], O. Todorovik[b], A. Selenica[c]

[a]National Institute of Meteorology and Hydrology, BAS
139 Ruski bld., 4001 Plovdiv, BULGARIA

[b]Hydrometeorological Service of Macedonia
Skupi bb, 1000 Skopje, MACEDONIA

[c]National Institute of Meteorology and Hydrology
Tirana, Albania

Abstract

The natural phenomenon of the Ohrid Lake has been investigated since the beginning of the XIX century. Its geological structure together with the geographical and political situation gathers the interest of scientists in a wide range of fields. However, only the recent advances in the physical modeling of the atmosphere and hydrosphere will permit the deeper understanding of the processes that occur between the lake Ohrid basin and the atmosphere. In the first part of the investigation ISBA land surface scheme is used to determine the water and energy budget on a single site. The aim of the second part is, using different sources of data and various techniques to evaluate the monthly water budget of the lake Ohrid and to compare the results to those of other investigations.

Keywords: SVAT modeling; Water balance; Water and energy budget.

Part A) Water and Energy budget of a land site near the lake – the Ohrid meteorological station

1. Introduction

a. Geographical and hydrographical characteristics

The Ohrid Lake is one of the eight oldest lakes in Europe. Its tectonic origin and the karstic geological structure of the surrounding mountains are the basis of its particular hydrological regime. The average volume of the lake is around 50.8 km^3, maximal depth of 289 m and surface of about 358 km^2. The lake has a relatively very small basin surface – 680 km^2 (Stankovik, 1959), compared to its water inflow. The obvious reason seems to be the underground inflow from the nearby Prespa Lake (853 m.a.s.l.) situated 158 m above the Ohrid Lake mean level (695 m.a.s.l.), through the Galicica and Suva Gora mountain karstic massifs. The last investigations show that about 50% of the water in the Saint Naum and Tushemisht springs on the south coast of Lake Ohrid is from Lake Prespa (Watzin et al., 2002). Since 1962, as a result of an intergovernmental decision between Albania and former Yugoslavia, in order to ensure the efficient hydropower production, the lake's water level is maintained between 691.65 and 693 m. This is achieved by controlling the water outflow to the river Crn Drim at the gate of Struga. This is the only water outflow from the Ohrid Lake; with an annual average of 22 m^3/s (Watzin et al., 2002). Water residence time of the Ohrid Lake is estimated between 60 and 85 years. This increases the dangerous effect of human activities in the basin, like release of unthreaded sewage waters and subsurface inflow of polluted irrigation water.

b. Climatic characteristics

The geographical situation of the lake between the mountain Galicica from the Macedonian eastern side, Mali i Tate as well as Guri i Kajes massifs from the Albanian south and western side, together with the nearness of the Adriatic Sea determine the mild climate of the region. Furthermore, because of its big thermal capacity, the lake is contributing to the lowering of temperature extremes. The monthly mean temperature at Pogradec, at the south coast, is between 2.1 in January and 20.8 ºC in July. The average annual temperature and relative humidity of the air in Ohrid are respectively 11.1 ºC and 70%. The basin of the lake has pronounced Mediterranean pluviometric regime. The maximum of the precipitations are in the winter, while the yearly average for Ohrid site is about 700 mm (Watzin et al., 2002). Precipitation totals are highly dependant on the topography.

2. The model used

The ISBA surface scheme (Interface Soil-Biosphere-Atmosphere) was developed for the climate, mesoscale and prediction atmospheric models used at Météo-France (Noilhan and Mahfouf, 1995). It aims to represent the main surface processes in a relatively simple way: it solves one energy budget for the soil and vegetation continuum, and uses the force-restore method (Deardorff, 1978) to compute energy and water transfers in the soil. The model takes as input the precipitations, air temperature, air specific humidity, wind velocity, global irradiance and atmospheric (long wave) irradiance. Vegetation is considered through its monthly changing parameters: vegetation fraction (veg), leaf area index (LAI), roughness length (z_0) and albedo. Evapotranspiration is computed through four components: interception by the foliage, bare soil evaporation, transpiration of the vegetation (with a stress function computed using the method proposed by Jarvis (1976)) and sublimation of the snowpack. After the energy budget is solved (computing of latent heat of evaporation – E, turbulent heat flux H and ground heat flux G), two fluxes of water in the soil are computed: a surface runoff (Qr) and drainage (D) (Figure 1). ISBA was coupled with the distributed hydrological model Modcou (Habets et al. 1999b). The last version of the model (Boone et al., 2000) uses 3 layers in the soil and 3 layer snow pack, which permits more detailed parameterization of the physical processes occurring at the screen level (first atmospheric level).

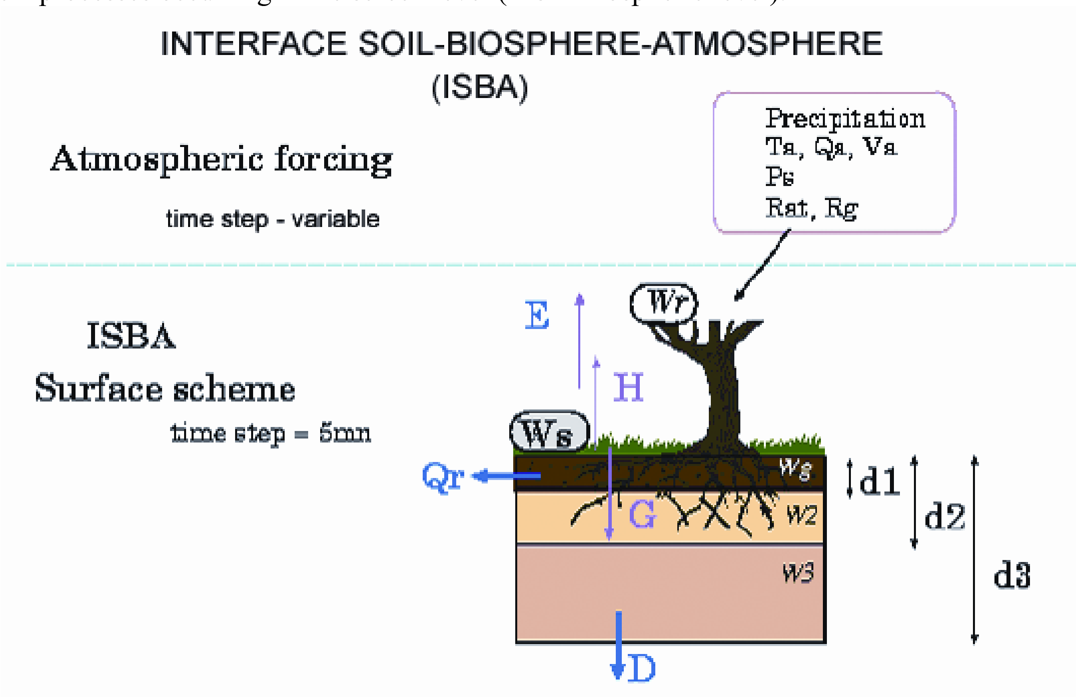

Figure 1: *ISBA land surface scheme*

3. Database of meteorological, hydrological, soil and vegetation data

Meteorological and hydrological information about the Ohrid Lake basin was collected from the Hydro-Meteorological Institute of Former Yugoslavian Republic of Macedonia (FYROM) and the Hydrometeorological Institute of Albania. In this first part of the study, only data from the Macedonian side for the year 1990 were used. The list of available data and the corresponding time step and stations are given in table 1.

Meteorological Parameter	Time Step	Station
Precipitations [mm]	24 h	Ohrid, Kuratica, Openica, Peshtani, Radolishta, Saint Naum
Snow pack height [cm]	24 h	Ohrid
Air Temperature [ºC]	1 h	Ohrid
Air relative moisture [%]	1 h	Ohrid
Wind velocity [m/s]	1 h	Ohrid
Nebulosity [1/8]	1 h	Ohrid, Bitola
Sunshine rate [1/10]	1 h	Ohrid, Bitola
Global Radiation [J/cm^2]	1 h	Bitola
Air Pressure [mb]	1 h	Ohrid
Streamflow discharge [m^3/s]	24 h	Lozani – river Crn Drim
Water Surface Temperature [ºC]	Instant	Ohrid (93 measurements for the period 1978-1992)
Air temperature [ºC]	Instant	Ohrid (93 measurements for the period 1978-1992)
Lake's water level	Monthly	Ohrid

Table 1**:** *List of available meteorological and hydrological data*

a. Meteorological data verification and correction

i. Verification of atmospheric pressure, air temperature, air relative moisture, wind velocity, cloudiness and hourly sunshine rate

Data from the main synoptical station of Ohrid is measured (observed) at hourly time step. It was first checked whether the data series of air temperature, air relative moisture, atmospheric pressure and wind velocity belong to the min - max interval of possible values, then data were compared to the 24 hours moving average, which permitted visual errors detection (figure 2). The small time step of one hour permitted to fill up the resulting gaps using linear interpolation (figure 3). Data series of sunshine rate and nebulosity were checked with logical test against the min-max envelope of each of them (0 to 9 for nebulosity; 0 to 10 – sunshine rate). As cloudiness is not observed during the night and early morning filling the missing data of nebulosity was made with linear interpolation. Missing data of sunshine rate were completed using a parameterization relating the hourly sunshine rate to the cloudiness, air temperature and solar declination. More precise evaluation of that parameter could be made by use of MNT, which would include the overshadowing effect of the surrounding terrain (Chen Xioafeng, 1996).

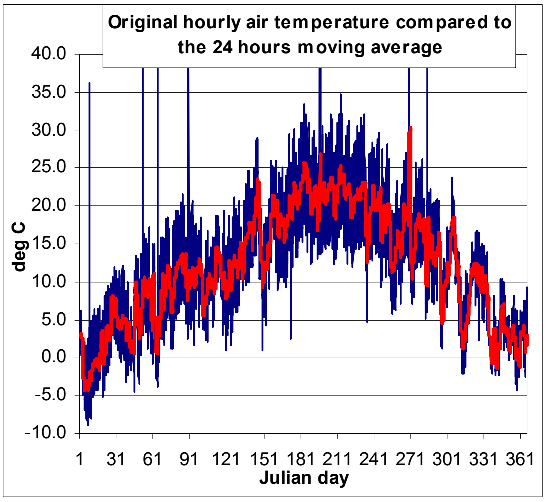

Figure 2: Original data series of hourly air temperature compared to the 24 hours moving average.

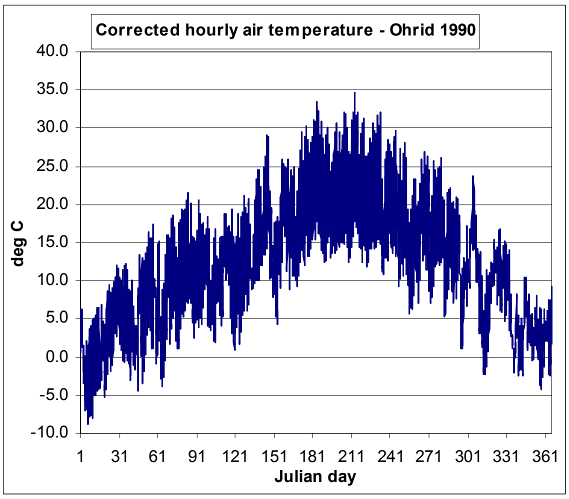

Figure 3: Corrected data series of hourly air temperature – Ohrid, year 1990.

b. Data series of shortwave global radiation, long wave atmospheric radiation and water temperature at hourly step

i. Computing of the global shortwave radiation

Data series of hourly shortwave radiation were derived with respect to the clear sky global irradiation, observed hourly sunshine rate and cloudiness. The first variable was calculated using the algorithms included in the Heliosat II software. The modeling of the irradiation for clear skies in that software originates from the clear-sky model of the European Solar Radiation Atlas (ESRA 2000; Rigollier *et al.* 2000) with corrections for the site elevation proposed by Remund, Page (2002). The monthly values for the Linke turbidity factor needed for the computing of the hourly irradiation series were obtained from the SoDa web service, supported by the European Commission (project SoDa, contract DG "INFSO" IST-1999-12245, http://www.sodais.com). To parameterize the global solar radiation a modified version of the equation of Kasten and Czeplak (1979) was used which estimates the global irradiation by use of the clear sky global irradiance and the cloudiness. The modification takes also into account the hourly sunshine rate (Artinyan, 1996). First data of hourly sunshine rate and cloudiness for Bitola, which is the only station with irradiation records nearby, were used to calibrate the equation's coefficients. It was found that, about 30% of the measured values are higher than the computed clear sky irradiation while using Linke turbidity factor equal to 1. Because of that, calibration of the equation 1 was made assuming a constant Linke turbidity factor (=1), while the final computing of Ohrid's site hourly global irradiation was made with respect to the mean monthly Linke turbidity factor. The equation is:

$$R_g = R_{g0} \times \left(a \times \left(1 - b \times P_C^{\,3.5} \right) + c \times P_S \right) \qquad (1)$$

where: R_g – hourly global irradiation in all weather conditions [Wh/m^2]; R_{g0} - hourly clear sky irradiation computed by the ESRA model with respect to the site coordinates and altitude and the monthly mean Linke turbidity factor for the given site [Wh/m^2]; P_c – parameter of cloudiness 0.0 to 1.0 [-]; P_s – parameter of the hourly sunshine rate 0.0 to 1.0 [-]; *a, b, c* – are regression coefficients, dimensionless.

For the area of South-West Macedonia the calibration of equation 1 led to the following values of the coefficients: $a = 0.485$; $b = 0.379$; $c = 0.516$.

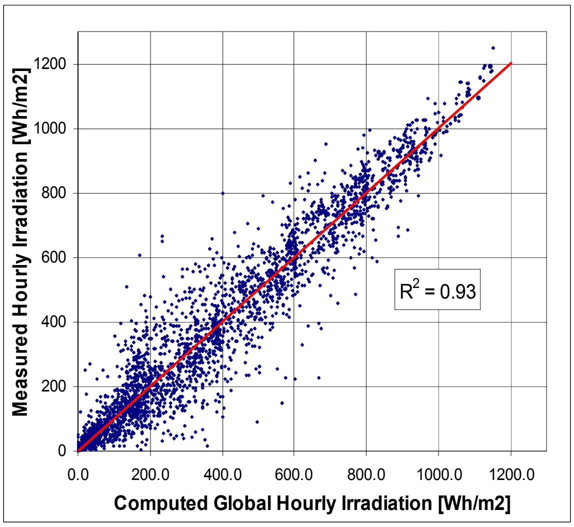

Figure 4: Comparison between computed by use of formula 1 and measured global irradiation for Bitola – 1990.

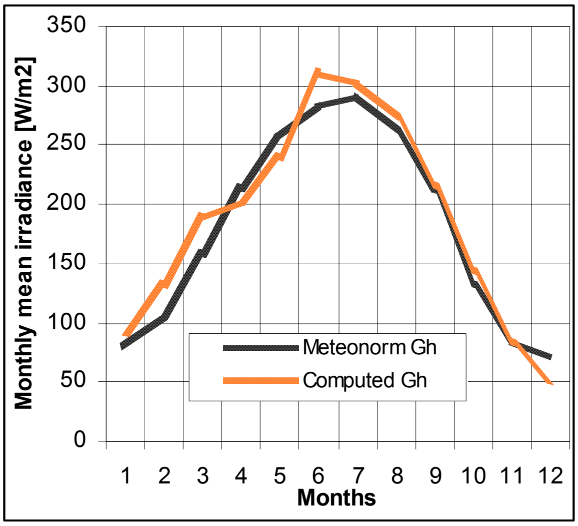

Figure 5: Comparison between computed with formula 1 and given by Meteonorm (ESRA model) monthly mean irradiance - Ohrid site, year 1990.

The computed square correlation and RMSE (root mean square error) are R^2=93% and 79 [Wh/m^2] respectively (figure 4). The equation coefficients show that computed values for clear sky conditions will give 100% of the ESRA model hourly clear sky global irradiation, 30 % of the clear sky irradiation with full cloud cover condition and 72% of the clear sky irradiation when half the sky is cloud-covered and 1/2 hour sunshine is observed. The resulting monthly mean irradiation showed results close to the climatological values given by Meteonorm database (www.meteotest.ch) (figure 5).

ii. Computing of the down welling atmospheric radiation

The ISBA land surface scheme uses the atmospheric radiation, in order to compute the radiation balance at the ground surface. Hourly step atmospheric radiation was computed according to the equation of Staley and Jurica, (1972). To estimate the atmospheric radiation, it considers the values of air temperature, specific humidity and cloudiness (equation 2). Specific humidity is computed from the air pressure, air temperature and air relative humidity.

$$R_{AT} = \left\{\sigma_C + (1-\sigma_C)\times 0.67\times\left(1670\times q_a\right)^{0.08}\right\}\times\sigma\times T_A^4 \qquad (2)$$

where R_{at} is the atmospheric irradiance [W/m^2], σ is the Stefan-Boltzmann constant, T_a and q_a are the air temperature [K] and specific humidity [-], σ_c is the cloud coverage ($0 \geq \sigma_c \geq 1$).

iii. Estimation of the water surface temperature

To evaluate the lake's surface evaporation it is necessary to know water surface temperature. The available water surface temperature measurements of the Ohrid Lake together with the instantaneous air temperature measurements extracted from the www.woisydes.net web site database (data were supplied by the Macedonian Hydro Meteorological Institute), allowed establishing a regression (3) between the Julian day, the air temperature and the water temperature. The first was used to represent the yearly cycle of the sub-surface daily averaged water temperature, which follows with some delay the yearly cycle of the daily mean air temperature. As the yearly curve is not symmetrical a third degree polynomial was used. Hourly air temperature was used to reproduce the fluctuations around the mean value. It was found that Julian day together with the hourly air temperature are sufficient to estimate the regression coefficients with a square correlation R^2 = 87% and RMSE of 2.2 [ºC]. The resulting equation is:

$$T_W = \left(a \times J^3 + b \times J^2 + c \times J \ + d\right) + f \times T_A \qquad (3)$$

where T_W is the hourly water surface temperature [ºC], T_A the air temperature [ºC], J is the Julian day and *a, b, c, d* are the equation coefficients [-]. The equation coefficients for computing the Ohrid Lake's surface water temperature are: *a* = -1.96E-6; *b* = 7.65E-4; *c* = -3.00E-2; *d* = 4.41; *f* = 3.72E-1. The measured and the computed values are shown with the time scale at figure 6. Using this equation to compute the surface water temperature presumes ignoring periodic mixing of surface and deep water layers. This is possible because they occur rarely – roughly once in 7 years (Hadzisce, 1966) and mostly in winter months when the surface temperature is near to the deeper water temperature. That error would not affect the evaporation computing. However it is important to mention that for the computing of the water surface temperature is needed the air temperature at measured at 2 m above water. That is not the case with the Ohrid station, which is situated 65 m above water mean level. That is, before the computing, the air temperature should be corrected with a factor accounting for the elevation difference.

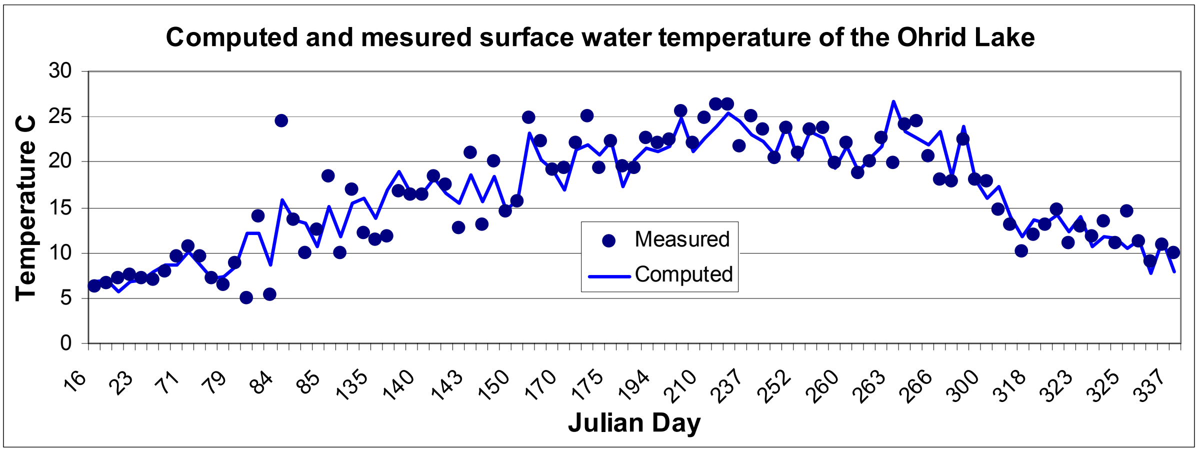

Figure 6: *Computed with equation 3 and measured water surface temperatures of the Ohrid Lake between 1978 and 1992 years (93 records).*

c. Vegetation and soil properties

The vegetation properties for the Ohrid site were found on the base of the land cover map for southern Europe in the Year 2000 (J-F.Pekel et al., 2003) (figure 7). According to the vegetation classification linked to the map, the Ohrid station area is characteristic with "cropland, rain fed cultivation" and "shrub cover, open evergreen". The dominant shrub vegetation types in the area are *Cupresus arisonica, var. piramidalis*, *Syringa vulgaris* etc. The vegetation map is given in figure 8 and the legend in table 2. The set of monthly changing parameters of the corresponding cell (cropland C3) with size 30" extracted from ECOCLIMAP (Champeaux, 2003) are described in table 3.

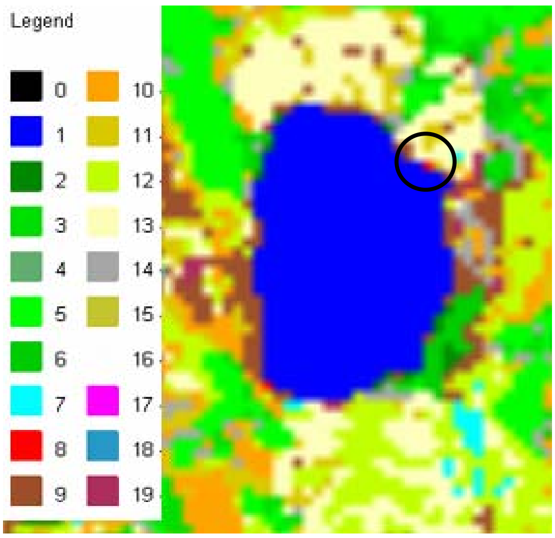

Figure 7: *Vegetation type map of Ohrid Lake's Basin*

N	Vegetation type
1	Water Bodies
2	Tree cover, Closed evergreen needle leaved
3	Tree cover, Broadleaved, deciduous
4	Tree cover, Needle leaved, evergreen
5	Tree cover, Closed deciduous, broadleaved
6	Tree cover, Mixed phenology or leaf type (50/50%)
7	Bare Areas (soil / Rock)
8	Urban Areas
9	Shrub Cover, closed evergreen needle leaved
10	Shrub cover, Dense to open deciduous broadleaved
11	Shrub cover, Open evergreen
12	Grassland, Herbaceous, closed-open
13	Cropland, Rain fed cultivation
14	Mosaic (Tree cover open deciduous forest / Shrub cover)
15	Mosaic (Tree cover / Natural Vegetation)
16	Snow
17	Wetland
18	Cropland, Irrigated
19	Cropland, Wooded (Olive and fruit trees etc)
20	Mosaic (Natural vegetation / Cropland)

Table 2: *Legend to the vegetation map*

Param.	Jan.	Feb.	Mar.	April	May	June	July	Aug.	Sep.	Oct.	Nov.	Dec.
veg $_{[-]}$	0.38	0.54	0.66	0.72	0.78	0.57	0.45	0.38	0.34	0.34	0.3	0.26
Lai $_{[m^2/m^2]}$	0.8	1.3	1.8	2.1	2.5	1.4	1	0.8	0.7	0.7	0.6	0.5
$z_{0\,[m]}$	0.02	0.02	0.04	0.04	0.06	0.03	0.02	0.02	0.02	0.02	0.01	0.01
$z_{0h\,[m]}$	2e-3	2e-3	4e-3	4e-3	6e-3	4e-3	2e-3	2e-3	2e-3	2e-3	1e-3	1e-3
albedo $_{[-]}$	0.15	0.17	0.17	0.18	0.18	0.17	0.16	0.15	0.15	0.15	0.15	0.14
$R_{smin\,[s/m]}$	40											

Table 3: *Monthly changing values of the vegetation parameters: veg (vegetation fraction – 0 to 1), Lai (leaf area index – that is, area of leaves per unit area of ground), z_0 (roughness length) for cropland cover (C3), z_{0h} roughness length for heat and the constant minimum stomatal resistance - R_{smin}.*

The dominant soil types are kalkomelanosol and rendzine. Their texture is described as sandy-clay. *Rendzine* and "on chalk" soils have an upper limit of volumetric moisture of 40% and field capacity up to 37%, but typically 30% (INRA, 1997). Soil parameters used by ISBA are sand and clay content in percents, soil and rooting depths. The values in table 4 that were extracted from ECOCLIMAP database originate from the FAO database with resolution 10 km, concerning the mechanical structure and from the vegetation map concerning the soil and rooting depth. The extracted texture data is pointing to the sandy-loam class (coarse to medium/coarse) (Cosby et al, 1984). Unlike the texture properties, the soil and rooting depths are not realistic for that type of soil, they were chosen according to 'in situ' observations.

Origin	Soil depth	Roots depth [cm]	Sand [%]	Clay [%]	Humus [%]
ECOCLIMAP	150	100	65	12	-
Observation	70	40	-	-	3 – 20 %

Table 4: *Values of the soil parameters: soil and roots depths, sand and clay percentage and humus content.*

4. Modeling results for the land site

a. Monthly water budget

The land water budget has the typical distribution of a Mediterranean climate site. The most of the precipitations fall in the winter (figure 8), when is occurring 69% of the total surface runoff and 100% of the yearly drainage (feeding riverflow through the soil column). A second maximum of precipitations appears in April but it is not resulting in riverflow because of the increased plant water demand in that time.

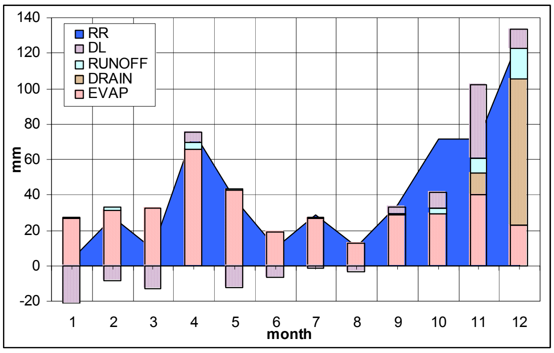

Figure 8: *Monthly water budget of the land site: RR - monthly total of precipitations; EVAP - monthly total evaporation; DRAIN - monthly total drainage and RUNOFF - surface runoff; DL – monthly average storage in the soil column [mm].*

Light snowfall occurred only in 11 days during February and December. Drainage is null during 10 months and on yearly basis represents only 19% of the precipitations (100%). The precipitations, snowmelt included, that are entering the soil (89%) are either used by plants for transpiration (26%) or evaporated from the bare soil (44%). The surface runoff (7%) is linked to the daily precipitation duration (intensity). As this parameter is not known, an average 6 hours per day precipitation forcing was used, when daily precipitation was measured. For comparison a test with 24 hours repartition of the daily rain was performed. It showed a relative increase of the evaporation of 4%. That rise of total evaporation is causing a smaller annual runoff of about -10% compared to the "6 hours long" daily rainfall.

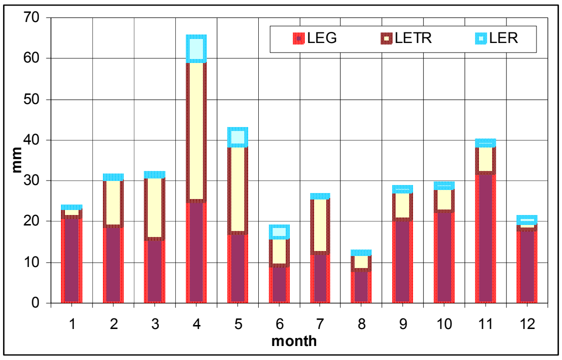

Figure 9: *Monthly totals of the components of the evaporation: LEG - bare soil, LETR - transpiration, LER - interception [mm].*

Evaporation (figure 9) is following the water availability in the soil. It depends partially from the soil depth, as deeper soil in general is storing and evaporating at higher rates. In the spring a little rise of the transpiration part of the total evaporation is seen. The reason is the lack of water for evaporation in the time when plant's water demand is higher. C3[1] type plants have higher water use in spring, as can be seen in table 3, when the density (veg) and leaf area index (LAI) are higher.

b. Monthly energy budget of the land surface

Land energy budget is characteristic with the yearly prevailing sensible heat flux (figure 10). That is explained with the lack of water for evaporation and so the smaller flux of the latent heat of evaporation. Net radiation is following the energy input rate – lowest in the winter and higher in the summer months. Ground heat transfer has small impact on the overall energy budget. A very different partitioning is seen above the water (cf. next paragraph).

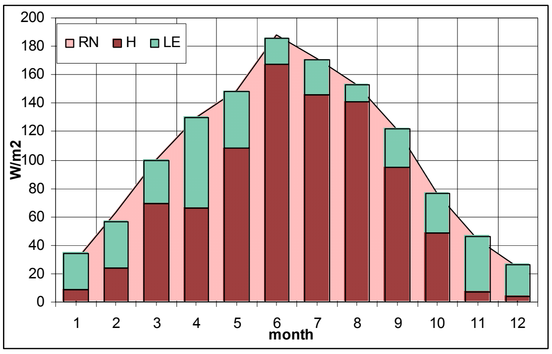

Figure 10: *Monthly average energy budget of the land site: RN - monthly average net energy flux; H - monthly average sensible heat flux; LE - monthly average latent heat [Wm^{-1}]. Storage term is neglected.*

Higher latent heat flux is observed in April when the growing vegetation is using the total available water and in November, which is due to the evaporation from bare ground.

[1] C3 and C4 grasses use different chemical pathways for photosynthesis and therefore respond differently to the environment. Most plants (including trees and shrubs) use the C3 pathway, but the C4 pathway is used by many tropical grasses and some important crops (e.g. Maize).

5. Modeling results for the lake water surface

a. Monthly energy budget of the water surface

ISBA land surface scheme incorporates a module for computing the water surface energy fluxes. It computes also the evaporation from the water surface. The input variables are the same meteorological data as for the land energy budget evaluation but water surface parameters and water surface temperature are used also. In general in NWP models, water surface temperature is assumed to be constant which leads to high modeling errors in areas with lakes. For the purpose of that application two modifications were introduced in ISBA: variable water surface temperature, and variable water surface albedo. Water surface parameters are described in table 5. ISBA uses Charnock's relation for water surface roughness length estimation. Water surface temperature is forced with computed values according to equation 3.

parameter	ISBA original	modified
water surface temperature	constant	variable
water surface roughness length	$z_{0sea} = 0.015 \times \frac{u_*^2}{g}$	same
water visible albedo	0.07	variable
water emissivity	0.98	same

Table 5: *Water surface parameters used in ISBA*

Water surface albedo is varying with the Julian day according to the formulation used in DYRESM - Dynamic reservoir simulation model (Antenucci and Imerito, 2002). Latent heat flux is computed according to the equation:

$$LE = \rho_a \times L_e \times D_h \times V_{mod} \times (q_{sat} - q_a) \quad (5)$$

LE is the flux of latent heat from the water surface [W/m^2]; ρ_a is the density of the air; L_e is the latent heat of vaporization (2.5E6); D_h is the drag coefficient for heat; V_{mod} is the wind speed module at the first atmospheric level [ms^{-1}]; q_{sat} and q_a are respectively the saturated and the specific moisture of the air [kg/kg].

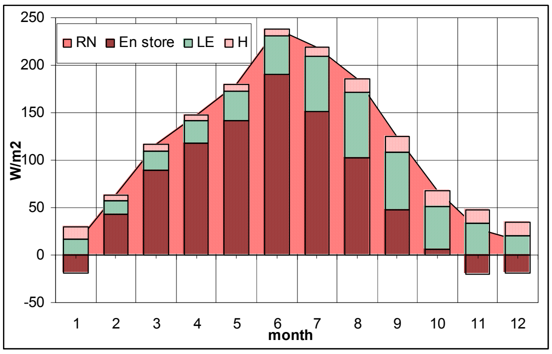

Figure 11: *Monthly average energy budget of the water surface computed by ISBA: RN - monthly average net energy flux; En store - monthly average energy storage; LE - monthly average latent heat; H - monthly average sensible heat flux; [Wm^{-1}].*

At figure 11 are shown the monthly components of the energy budget above the water surface computed by ISBA. In opposite to the land energy budget (figure 11) here the largest part is taken by the storage term. The yearly graph shows a slow rise of the latent heat flux in the spring, higher values in July, August and September and persistent values in autumn. The yearly average energy storage is 70W/m^2. The lake collects energy during the spring and summer and expends it during the fall and winter.

b. Monthly evaporation from the lake

The open water evaporation is function of atmospheric and physiographic conditions different from those that are measured (observed) at a land meteorological station. By instance temperature of the water at the surface (and vapor pressure above water surface), is linked to the air temperature but also is following the annual rhythm of the deep water temperature depending on the heat capacity of the lake, the horizontal and vertical fluxes of movement and heat in the lake itself etc. An estimate of the lake evaporation was made using two different methods for comparison: by the ISBA land surface scheme and using the DYRESM software and the same meteorological data set. DYRESM-CAEDYM is a coupled hydrodynamic - ecological model CAEDYM (Computational Aquatic Ecosystem Dynamic Model). DYRESM predicts the variation of temperature and salinity with depth and time. The formulation for the latent heat evaluation used by DYRESM software (Fischer et al. 1979 eqn 6.20) is near to that used by ISBA : eqn.(6)

$$Q_{lh} = \min\left\{0, \frac{0.622}{P} C_L \rho_A L_E U_a (e_a - e_s(T_s))\Delta t\right\}$$

where P is the atmospheric pressure in hectopascals, C_L is the latent heat transfer coefficient (=1.3x10^{-3}) for wind speed at 10 m reference height above the water surface, ρ_a the density of air in kg/m^3, L_E is the latent heat of evaporation of water (= 2.453x106 J/kg), U_a is the wind speed in m/s at the reference height of 10 m, e_a the vapor pressure of the air, and es the saturation vapor pressure at the water surface temperature T_S; both vapor pressures are measured in hectopascals. The simulation with DYRESM was performed with the assumption of equal (and very small) inflow and outflow. That permitted to have a relatively constant free water surface so the changes in the lake level height are only function of the evaporation and the precipitation. The sum of decreases of the level within a month is considered to be equal to the monthly evaporation total.

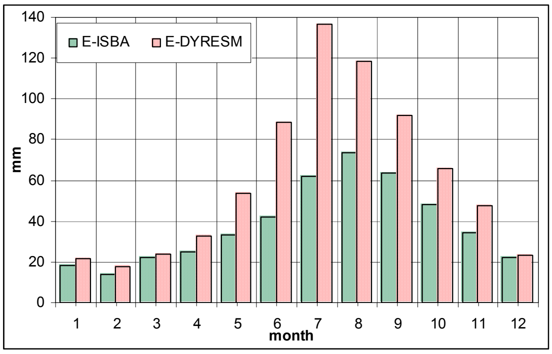

Figure 12: *Monthly sum of the evaporation from the water surface computed by ISBA and by DYRESM [mm]*

The two models are producing the same shape of the yearly evolution of the evaporation (figure 12); however the values of ISBA are lower with an average factor of 1.6. The corresponding results of yearly total evaporation are 453 mm – computed with ISBA and 722 mm computed with DYRESM. Although the second value is the most probable the final conclusion should be made when in-situ .observations of the lake water surface evaporation will be obtained.

Part B) Estimation of the lake monthly water budget for 1990

6. Monthly water budget of the Ohrid Lake for 1990

The water budget of lakes is based on the mass conservation law and has the form of a balance equation:

$$\frac{dV_L}{dt} = I_s + I_g + P - O_s - O_g - E \qquad (7)$$

V_L is the lake volume (Figure 13), I_S, I_G, O_S and O_G represent the volumetric surface and groundwater inflow and outflow fluxes, respectively, P is the precipitation over the lake and E is the evaporation flux from the lake. Parameters in Eq. 7 are functions of time. The water density is assumed constant. To derive any given component of the water budget (e.g. the rate of groundwater inflow) from Eq. 7, all other parameters have to be known or to be obtained from independent estimates (Rozanski et al., 2000). In the case of Ohrid Lake the term $D_v = \frac{dV_l}{dt}$ could be derived from the level-volume rating curve (storage table).

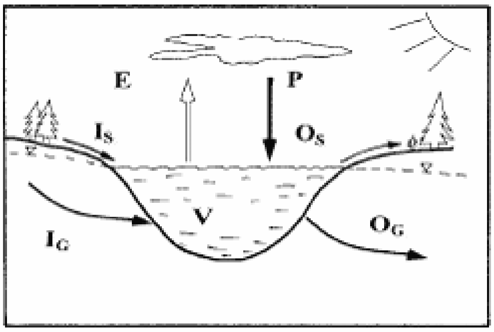

Figure 13: Schematic diagram showing components of hydrologic budget of a lake system.

If underground outflow is neglected, outflow is equal to the Crn Drim River stream flow. That is, if evaporation and precipitation over the lake are computed, the sum of remaining terms (surface and groundwater inflow) can be evaluated. Furthermore, applying ISBA at the basin scale could be estimated the surface inflow and as unknown term of the equation - the underground inflow which comes from Prespa Lake.

c. Water outflow through the Crn Drim River

The term of the surface outflow (O_s from the Eq. 7) is determined from the streamflow discharge of the only river that takes it beginning from the Ohrid Lake – the river Crn Drim. The mean annual discharge of Crn Drim is evaluated about 22 m^3/s (Watzin et al., 2002) but for the year 1990 is computed a lower value - 14 m^3/s. Monthly mean streamflow discharge is given at the figure 14.

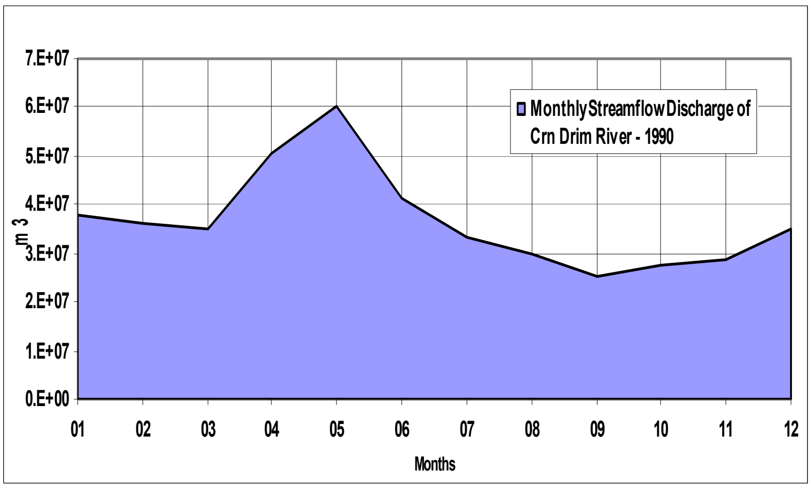

Figure 14: Monthly streamflow discharge [m^3] for 1990. Crn Drim River at Struga station.

d. Lake storage variability

As mentioned before, variations of the lake's volume could be evaluated using a rating curve relating the measured levels to the lake's volume. To do that the bathymetric map published by Stankovik (1959) was used. It was scanned, vectorized and scaled in appropriate way in order to compute the volumes and water surfaces at different levels (Figure 15). Then with the resulting couples level-volume and level-surface were drawn the rating curves for volume and open water surface (Figure 16).

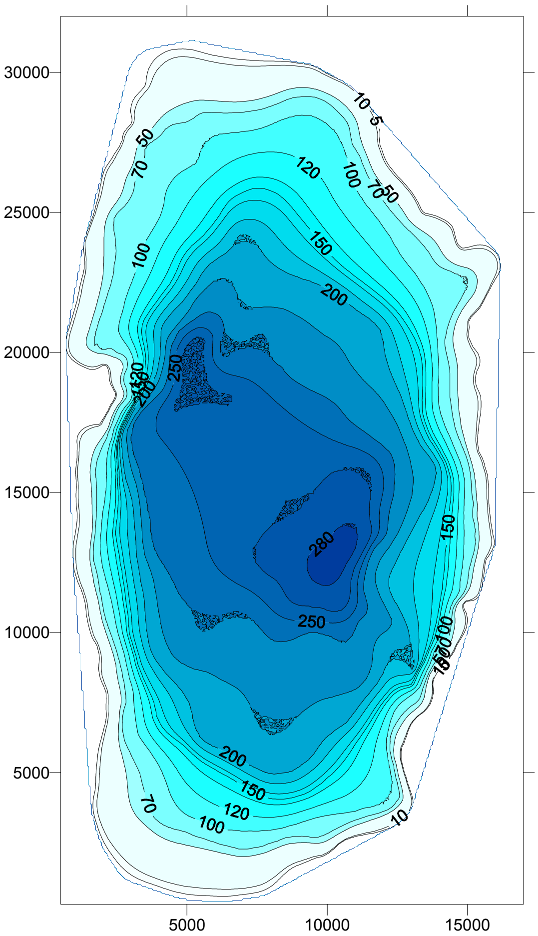

Figure 15: *Bathymetric map of the Ohrid Lake (*Stankovik, 1959*). Scale in m.*

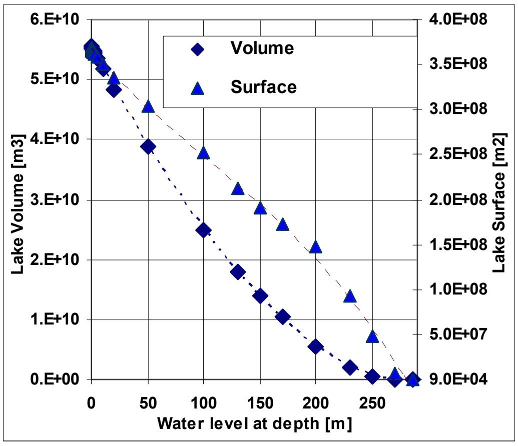

Figure 16: *Morphometric curves for volume and surface of the Ohrid Lake, derived from the bathymetric map.*

In the upper part of the curve, which has linear shape, both for volume and surface, the slope is only determining the volume difference between two levels. That permitted to convert the monthly mean water levels of the lake recorded at Ohrid hydrological station into monthly variation (the term $D_v = \frac{dV_l}{dt}$ from eq. 7) of the lake's volume and surface (Figure 17).

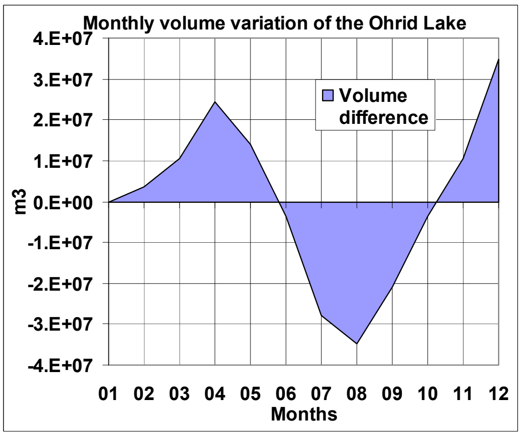

Figure 17: *Monthly volume variation of the lake [m^3] for 1990.*

e. Estimated precipitations over the lake

From the available precipitation stations (table 1) were extracted the monthly and the yearly total precipitations. They were compared with the published values of those stations (Watzin et al, 2002) and also of the stations of Struga and Pogradeci. A simple relation is built in order to estimate the missing values for 1990 for Struga and Pogradeci. The results for the annual sum are given in table 6. The averaged monthly partitioning of precipitations for 1990 is applied for the yearly sum of 517 mm at the figure 18.

Station	Altitude	Sum 1990	Average annual sum
Sv.Naum	698	572	888
Peshtani	720	472.1	728
Struga	695	"527"	794
Pogradeci	-	"507"	748
Ohrid	760	509	703
Average		517	772

Table 6*: Annual sum of precipitation from the shoreline rainfall stations. The values in quotes are estimated with a linear relation.*

f. Estimated monthly totals of the water inflow

Previous investigations (Watzin et al., 2002) found that mean annual surface inflow to the Ohrid Lake is about $456.3 \times 10^6 m^3$. The total inflow is estimated about $780.3 \times 10^6 m^3$. The same paper reports as mean annual precipitation in the lake proximity the value of 772.5mm. Comparing these results to the findings above it becomes clear that 1990 is a dry year with 67% of the average year's sum of precipitations. Ignoring the non-linearity of the natural processes, if we reduce the above discharge volumes with respect of the precipitations difference, the values for the surface and total inflow are respectively: 305 and 522 $\times 10^6 m^3$ (for 1990). The last number is confirmed by the computed in the present investigation total inflow - 521 $\times 10^6 m^3$.

Month	*P*	*E*	*O*	D_v	*I*	Lake surface m^2
1	4.2	21.8	105.4	0.0	123.1	357.9E6
2	20.8	17.5	101.3	9.8	107.7	357.9E6
3	7.2	23.7	97.3	29.3	143.0	358.0E6
4	75.2	32.8	141.0	68.3	166.8	358.1E6
5	42.1	53.9	168.4	39.0	219.1	358.2E6
6	12.1	88.6	115.9	-9.8	182.6	358.1E6
7	18.2	136.6	92.9	-78.1	133.3	358.0E6
8	21.3	118.2	83.5	-97.6	82.8	357.9E6
9	45.1	91.9	71.2	-58.6	59.4	357.8E6
10	54.1	65.9	76.4	-9.8	78.4	357.8E6
11	76.5	47.8	79.8	29.3	80.4	357.8E6
12	140.1	23.5	98.0	97.6	79.0	358.0E6
Sum	517.0	722.1	1231.1	19.4	1455.6	
Sum m^3	185E6	258E6	441E6	699E6	521E6	

Table *7: Monthly sums of the water budget components: I – total inflow [mm]; O – outflow; P – precipitation over the lake [mm]; E – evaporation from the water surface [mm];* D_v *is the monthly change in the lake's volume computed from the measured monthly water level[mm].*

The monthly water budget of the lake Ohrid according to equation 7 is presented in the table 7 and the figure 19. The terms I_S and I_G that represent the surface and underground inflow are gathered together in the term *I*. O_G representing the underground outflow flux is assumed to be null, so the term is presented as *O*. The term D_v presents the variation of the lake's volume computed from the lake morphometry. All the values are presented in mm, except the last row that is in m^3. The values in mm should be reported to the variable lake surface, which values are given also in the table 7.

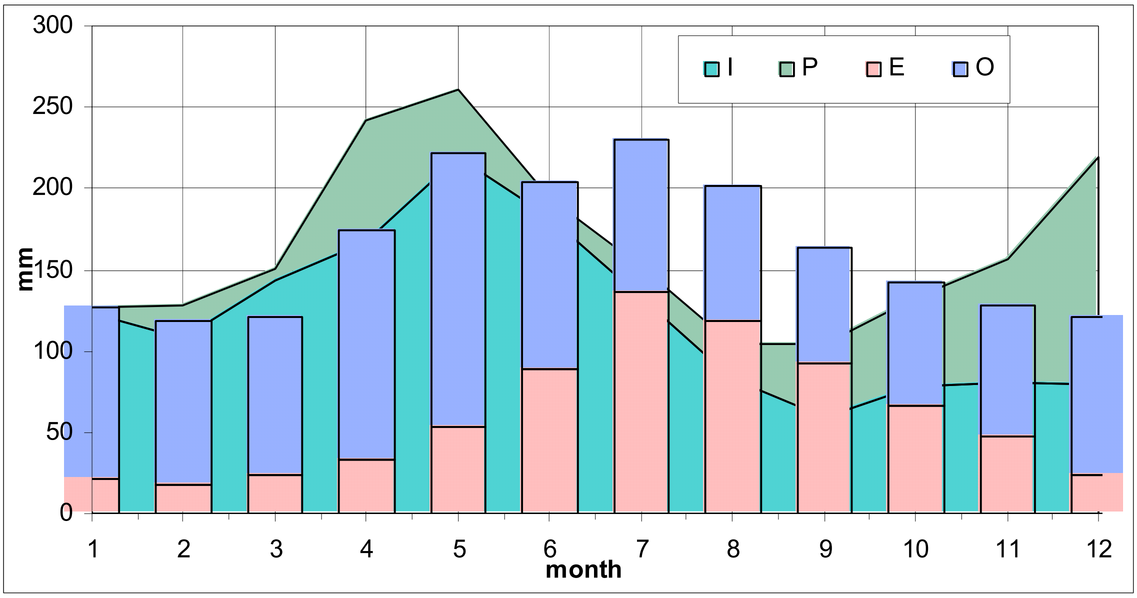

Figure 18: *Monthly water balance of the lake Ohrid for 1990. As stacked area are presented the positive terms of the budget: I – monthly total inflow [mm] and P –monthly sum of precipitation over the lake. As stacked columns are presented the negative terms of the budget: E – monthly sum of evaporation and O - outflow [mm].*

g. Discussion

The gathered data permitted to estimate the monthly partitioning of the water inflow of the lake Ohrid. Because of the large variety of processes with great number of parameters to assess, the methods for evaporation computing and water body volume approximation are not able to give enough reliable results. Although evaporation from the water surface is a largely investigated field, the various formulations are giving an error of about 10-20% (Gibson et al., 1996). It was found that the evaporation from the water surface is highly dependant on the water surface temperature. That parameter is in his turn dependant from the lake internal dynamics (mixing of the layers), the precipitations over the lake (amount and frequency) and the inflow volume and its temperature. In the case when no inflow and no precipitations are provided to the model (DYRESM) the water surface and subsurface temperature is raising subsequently and computed yearly evaporation sum is above 900 mm. Confirming the results is possible by comparing them to the in-situ measured values that is not always possible. As a result it is difficult to ascertain the remaining terms of the water budget with high level of probability. However, it remains possible to define their possible limiting values as function of the possible limits of the computed terms. The previously determined yearly sum of the evaporation (Watzin et al., 2002) from the lake's surface is 1146 mm. This value is 59% higher than the value computed in this work. That difference is bringing up the question of precise determination of the underground flow into Ohrid Lake, which is impossible to measure directly. The difference of 424 mm is near the sum of precipitations falling on the lake and 1/3 of the outflow. The computed in this work total inflow volume – $521x10^6$ m^3 has to be compared with total measured discharge into the lake for 1990 in order to confirm the partitioning between surface and underground feeding of the lake Ohrid.

7. Conclusion

h. Part A) Water and energy budget of a land site near the lake – the Ohrid meteorological station

In the first part of this paper was described the water and energy budget of the land site – Ohrid meteorological station. The land surface scheme ISBA allows estimating, with the use of physically based formulations, the partitioning of the precipitations into evaporation, drainage and surface runoff. It was found that most of the incoming solar energy is transformed into sensible heat flux, as not enough water is available for evaporation, except for a short period in the spring and late fall (figure 10). The prevailing part of the drainage and runoff for the year 1990 occurred in November and December as only in these months water availability was higher than the evaporation (figure 8).

i. Part B) Estimation of the lake monthly water budget for 1990

Figure 18 shows clearly the monthly partitioning of the lake water budget. The inflow is prevailing in winter and spring time and lower than the outflow during the summer (July, August, and September). The evaporation is slowly rising from January to May; has higher values in June to September; then still persists till November. The inflow is higher in spring months, while most of the positive part of the balance in winter is coming from the precipitations on the lake surface. That indicates possible underground feeding of karstic reservoirs in the surrounding mountains during fall and winter and consequently emptying into the lake during spring and summer months. These results should be confirmed after comparison with measured discharges of the main tributaries of the lake: the rivers Sateska, Koselska, Cerava, Pogradec, Verdova, but also with the springs discharge St. Naum, Biljana and Tushemisht.

8. Acknowledgments

The data for this study has been made available by the Institute of Meteorology and Hydrology of Macedonia, the WOISYDES project web site and personally by Mr. Agim Selenica from the Institute of Meteorology and Hydrology of Albania. The authors acknowledge these institutes for their support.

9. References

Artinian, E., 1996: Modélisation hydrologique du bassin du Rhône pour l'année 1987-1988. Rapport technique, CNRM/ENM. Rapport de stage de Mastère.

Boone, A., and P. Etchevers, 2000: An intercomparison of three snow schemes of varying complexity coupled to the same land surface model: local-scale evaluation at an alpine site. Journal of Hydrometeorology. August 2001.

Champeaux J.L., V. Masson 2003: ECOCLIMAP, a global surface parameters database at 1 km resolution derived from land cover and climatic maps – update with GLC2000. Global Land Cover 2000 "final results" workshop Ispra, 24-26 March 2003.

Chen Xiaofeng, Liu Jiyuan, Zhang Zengxiang, Peng Xulong & Liu Bin, 1996: Paper presented at the 4th International Symposium on High Mountain Remote Sensing Cartography, Karlstad - Kiruna - Tromsø, August 19-29, 1996

Cosby, B.J., G.M. Hornberger, R.B. Clapp, and T.R. Ginn, 1984: A statistical exploration of the relationships of soil moisture characteristics to the physical properties of soils, Water Resources Research, 20:682-690.

Deardorff, J.W., 1978: Efficient prediction of ground temperature and moisture with inclusion of a layer of vegetation. J. Geophys. Res., 83, 1889-1903.

Fischer, H. B., List, E. G., Koh, R. C. Y., Imberger, J., and Brooks, N. H. 1979: Mixing in Inland and Coastal Waters. Academic Press.
Food and Agriculture Organization (FAO) of the United Nations, 1970-78: Soil map of the world, scale 1:5,000,000, volumes I- X: United Nations Educational, Scientific, and Cultural Organization, Paris.
Gibson, J.J., Edwards, T.W.D. and Prowse, T.D., 1996: Development and validation of an isotopic method for estimating lake evaporation. Hydrological Processess 10: 1369-1382.
Golaz, C., and C. Cavazzi, 1995: Exploitation d'un modèle numérique du terrain pour l'aide á la mise en place d'un modèle hydrologique distribué. Rapport technique, CIG, Ecole des Mines de Fontainebleau. DEA d'hydrologie, Université PARIS 6. (in French)
Habets, F., J. Noilhan, C. Golaz, J. P. Goutorbe, P. Lacarrère, E. Leblois, E. Ledoux, E. Martin, C. Ottlé, D. Vidal-Madjar, 1999a: The ISBA surface scheme in a macroscale hydrological model applied to the Hapex-Mobilhy area Part 1: Model and database. J. Hydrol., 217, 75-96.
Hadzisce, S.D. 1966: Das Mixophänomen im Ohridsee im Laufe der Jahre 1941/42-1964/65. Verh. Internat. Verein. Limnol. 16: 134-138
INRA, 1997: Châlons Oilseed Rape Data Base / Environnement et Grandes Cultures / leviel@grignon.inra.fr (http://www-egc.grignon.inra.fr/ecobilan/base/CORD2.html)
Jarvis, P.G., 1976: The interpretation of leaf water potential and stomatal conductance found in canopies in the field. Phil. Trans. R. Soc. London, Ser. B, 273, 593-610.
J-F.Pekel, N.Vancutsem, P.Defourney, J-L.Champeaux, C.Gouveia, A.Lobo, S.Griguolo, A.Perdigao, E.Bartholome: The Land Cover Map for Southern Europe in the Year 2000. GLC2000 database, European Commision Joint Research Centre, 2003.
Kasten, F., and G.Czeplak, 1979: Solar and terrestrial radiation dependent on the amount and type of cloud, Solar Energy, Vol. 24, 177-189.
Noilhan J., and J. F. Mahfouf, 1995: The ISBA Land Surface Parameterisation Scheme. - In: Global and Planetary Change, vol. 13, pp 145-159.
Remund, J. and J. Page, 2002: Chain of algorithms: short- and longwave radiation with associated temperature prediction resources. SoDa Deliverable D5-2-2/3. Internal document.
Rigollier C., Bauer O., Wald L., 2000: On the clear sky model of the 4th European Solar Radiation Atlas with respect to the Heliosat method. Solar Energy, 68(1), 33-48
Rozanski K., Froehlich K., Mook W., Stichler W., 2000: UNESCO/IAEA Series on Environmental Isotopes in the Hydrological Cycle. Principles and Applications. Volume III: Surface Water. (url: http://www.iaea.or.at/programmes/ripc/ih/volumes/volumes.htm)
S.Griguolo, A.Perdigao, E.Bartholome, 2000: The Land Cover Map for Southern Europe in the Year 2000. GLC2000 database, European Commision Joint Research Centre, 2003.
Staley, D. and G. Jurica, 1972: Effective atmospheric emissivity under clear skies. J. Appl. Meteor., 11, 349-356.
Stankovik S., 1959: The Ohrid Lake and his live world. Kultura, Skopie, 1959 (in macedonian)
Watzin, M.C., V.Puka, and T.B. Naumoski, eds.2002: Lake Ohrid and its Watershed, State of the environment report. Lake Ohrid Conservation Project. Tirana, Albania and Ohrid Macedonia. 134 pp.